Available online at www.sciencedirect.com
SCIENCE DIRECT®
Plant Physiology and Biochemistry 42 (2004) 731–738
Plant Physiology and Biochemistry
www.elsevier.com/locate/plaphy

Original article

Over-expression of potato virus X TGBp1 movement protein in transgenic tobacco plants causes developmental and metabolic alterations

Ken Kobayashi [a,1,2], Catherine Sarrobert [b,1], Ximena Ares [a], María M. Rivero [a], Sara Maldonado [c], Christophe Robaglia [b], Alejandro Mentaberry [a,*]

[a] *Instituto de Investigaciones en Ingeniería Genética y Biología Molecular (CONICET), Facultad de Ciencias Exactas y Naturales (UBA), Vuelta de Obligado 2490, 1428 Buenos Aires, Argentina*
[b] *Laboratoire du Métabolisme Carboné, Département d'Écophysiologie Végétale et Microbiologie, Centre de Cadarache, CEA, 13108 Saint-Paul-Lez-Durance, France*
[c] *Facultad de Ciencias Exactas y Naturales (UBA), Ciudad Universitaria, 1428 Buenos Aires, Argentina*

Received 27 November 2003; accepted 23 July 2004

Available online 07 September 2004

Abstract

Transgenic *Nicotiana tabacum* plants expressing the TGBp1 movement protein of potato virus X (PVX) were studied to investigate the effects caused by this protein on plant physiology and development. TGBp1 caused consistent reductions of size and weight in different organs of these plants; however shoot-to-root ratios were similar to those of control plants. Transgenic seedlings showed smaller root meristems and calli derived from TGBp1 leaves grew at a slower rate through successive subcultures. Microscopic observations of TGBp1 plants revealed flattened chloroplasts containing plastoglobuli-like bodies. Further analyses showed a considerable reduction in photosynthetic rate, lower starch levels in leaves and roots, higher nitrate accumulation in leaves and induction of pathogenesis-related (PR) protein genes. Since these changes were not observed when other PVX sequences were expressed in tobacco, we postulate that TGBp1 is an important symptom contributor in PVX infections.

Keywords: Chloroplast; Movement protein; Physiology; Potexvirus; Tobacco

1. Introduction

Potato virus X (PVX) is the type member of the Potexvirus genus. The viral genome encodes five proteins: the viral replicase, three proteins involved in virus movement (TGBp1, TGBp2 and TGBp3) and the viral coat protein [14]. The proteins associated with viral movement are encoded by a block of three partially overlapped open reading frames termed the "triple gene block". Together with the coat protein, these proteins are required for viral movement. Studies on PVX TGBp1 (strain UK3) and the corresponding proteins of White clover mosaic potexvirus (WClMV) and Foxtail mosaic potexvirus demonstrated that these proteins can bind RNA, have ATPase and helicase activities, increase the plasmodesmata size exclusion limit, and move from cell to cell [1,15,20–23,31,35]. In addition, a suppression activity of post-transcriptional gene silencing has been also assigned to TGBp1 [37]. Both PVX TGBp2 and TGBp3 proteins are required for virus movement, but their precise functions are still unknown. It has been proposed that PVX moves from cell to cell as a ribonucleic acid–protein complex including the viral gRNA, the TGBp1 and the viral coat protein, and that the TGBp2 and TGBp3 proteins would act as docking proteins targeting this complex to the plasmodesmata [1,23,25,27,32,33,39].

A current model for plant–virus infections proposes that interference of symplastic transport by viral MPs could induce alterations in biomass partitioning, down-regulation of photosynthesis and, often, expression of defense-related

Abbreviations: MP, Movement protein; PR, Pathogenesis-related; PVX, Potato virus X; WClMV, White clover mosaic virus.

* Corresponding author.
E-mail address: amenta@dna.uba.ar (A. Mentaberry).

[1] Both authors contributed equally to this work.

[2] Present address: PMB UC Berkeley, USA.

0981-9428/$ - see front matter © 2004 Elsevier SAS. All rights reserved.
doi:10.1016/j.plaphy.2004.07.010

Table 1
Morphological parameters of 10 weeks old TGBp1 plants. Transgenic TGBp1 plants (A5, B16, C3, C6, D3, E2) and control (D8) tobacco plants. Internode length was determined dividing by four the distance along five mature successive leaves. Values represent the mean of triplicate determinations from a single representative assay. The assay was repeated two times with similar results. TGBp1 accumulation levels were determined by Western blot using polyclonal antibodies to PVX TGBp1

Plant	Height (cm)	Number of leaves	Internode [a] length (cm)	Leaf size [b] (cm)	Weight of shoots (g FW)	Weight of roots (g FW)	Shoot/root ratio [c]	p24 expression level [d] (%)
D8	64.0 (3.5)	16.0 (1)	6.7 (0.1)	19.5 (0.5)	90.5 (10.8)	4.7 (0.3)	19.4 (1.5)	0
A5	66.0 (3.2)	16.0 (1.5)	6.3 (0.3)	19.0 (0.9)	86.3 (9.0)	4.6 (1.0)	19.0 (2.6)	51
B16	52.3 * (1.5)	14.0 (1)	5.3 * (0.3)	18.8 (1.3)	75.7 9.0)	4.9 (0.5)	15.5 * (1.6)	70
E2	39.0 ** (3.8)	13.0 * (0.6)	5.0 ** (0.3)	16.3 ** (0.3)	56.3 * (2.7)	3.1 ** (0.3)	18.1 (2.3)	78
D3	35.3 *(5.8)	11.0 * (0.6)	5.2 (0.7)	17.2 * (0.8)	57.8 * (3.4)	2.7 * (0.2)	21.7 (0.6)	94
C6	33.0 * (4.2)	9.5 ** (0.7)	5.6 (0.6)	15.5 * (0.7)	36.3 * (3.5)	1.6 * (0.1)	23.1 * (1.7)	96
C3	22.0 ** (0.6)	11.0 ** (0.6)	2.9 ** (0.1)	13.2 ** (0.3)	29.5 ** (3.3)	1.5 ** (0.1)	19.7 (1.9)	100

( ): Indicates standard deviation. *: $P < 0.05$; **: $P < 0.01$ by Student's t-test.
[a] Distance between two mature leaves.
[b] Longitudinal length of mature leaf positioned in the middle of shoot. All leaves were equivalent.
[c] Shoot/root fresh weight ratio.
[d] Relative p24 protein accumulation in leaves determined by Western blot.

genes [11,12]. It was recently reported that expression of WClMV TGBp1 in transgenic *Nicotiana benthamiana* plants induces altered growth and plant development. Also, it was shown that constitutive expression of this viral MP in meristematic tissues—which are normally protected against virus invasion—induced abnormal leaf polarity and altered plant development [9]. It was concluded that this peculiar phenotype resulted from the interaction of the viral MP with components of the surveillance system controlling the selective entry of informational macromolecules into meristems. To our knowledge, there are very few, if any, systematic studies on the effects caused by PVX TGBp1 expression in host physiology. Although many advances have been made on the specific functions of potexviral proteins, the identity of those components inducing symptom development and disease-associated metabolic alterations remains still unclear.

In this work, we investigated the effects caused by the constitutive expression of the PVX TBGp1 sequence on the development and metabolism of transgenic *N. tabacum* plants. Several tobacco lines that were partially characterized in a previous work [2] were studied in further detail, revealing that TGBp1 expression induces consistent physiological changes. These changes include abnormal chloroplast functioning and altered metabolite contents and a lower cell division rate. Based on these results, we postulate that TGBp1 plays an important role in viral symptom formation.

2. Results

2.1. Morphological characterization of transgenic plants

Six tobacco lines showing a broad range of TGBp1 accumulation were compared (Table 1). Lines expressing high and intermediate TGBp1 levels displayed severe and moderate stunted phenotypes, respectively. Low TGBp1 expressers were indistinguishable from control plants. Highest TGBp1 expressers showed a distinctive phenotype consisting of shorter internodes, decreased leaf number and a slightly chlorotic appearance (Fig. 1A). Leaves, shoots and roots from these transgenic plants exhibit smaller sizes and lower fresh weights than those from control plants. These reductions seem to be correlated with TGBp1 levels (Table 1). Interestingly, shoot-to-root ratios were similar in TGBp1 and non-transgenic plants. On the other hand, tobacco plants transformed with the PVX TGBp2, TGBp3, viral replicase and coat protein genes showed a normal appearance as compared with their respective non-transformed controls ([17] data not shown).

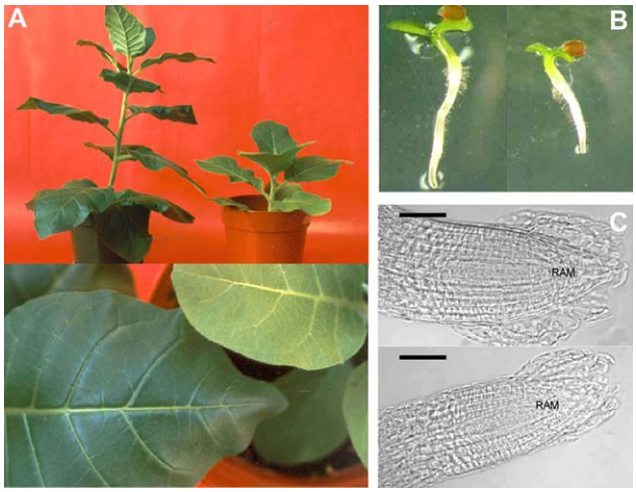

Fig. 1. Phenotypic characteristics of TGBp1 plants. **A**, TGBp1 phenotype. Upper panel: *N. tabacum* Xanthi D8 (left) and line C3 (right) plants at 8 weeks post-germination. Lower panel: leaves from the same plants. TGBp1 leaves (left) show a mild chlorotic aspect. **B**, Line C3 (right) and *N. tabacum* Xanthi D8 (left) plants at 5 d post-germination. **C**, Representative pictures of primary root meristems corresponding to *N. tabacum* Xanthi D8 (upper panel) and C3 (lower panel) plants at 5 d post-germination. Meristematic zones from control D8 and C3 plants exhibit mean volumes of 0.143 ± 0.017 and 0.091 ± 0.008 mm^3, respectively. Results are the average value from six individual root meristems. Root volumes were calculated as cylinders. Bar = 200 μm. RAM: root apical meristem.

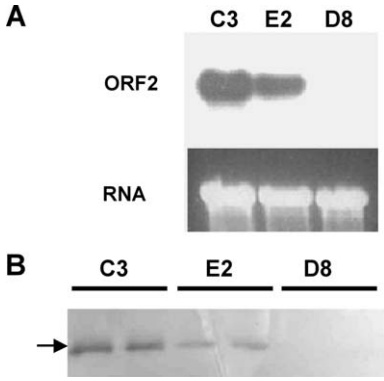

Fig. 2. Characterization of TGBp1 plants. **A**, Northern blot analysis of lines C3 and E2. Total leaf RNA from both lines and *N. tabacum* Xanthi D8 controls was obtained at 13 weeks post-germination. Five micrograms of total RNA were loaded in each lane. Position corresponding to the ORF2 transcript is indicated. Ribosomal RNA (loading control) is shown in the lower panel. **B**, Western blot analysis of C3 and E2 plants. Total protein extracts (30 μg per lane) from transgenic and control plant leaves were analyzed using polyclonal antibodies to PVX TGBp1 MP. The arrow indicates the band corresponding to PVX TGBp1 MP.

Two representative lines, C3 and E2, showing high and intermediate levels of TGBp1 accumulation (Fig. 2A, B) were chosen for further studies. Both lines exhibited consistently reduced sizes along all developmental stages, including those in which carbon autotrophy is not yet fully established (Fig. 1B). Smaller root meristems were observed in lines C3 and E2 in seedlings examined at 5 d post-germination (Fig. 1C and Fig. 3A–C). In both transgenic lines the root apical meristem (RAM) diameter averaged six to seven cells thick, whereas in the D8 control line this diameter averaged nine cells thick. In addition, cell size in control root meristem was slightly smaller than in transgenic lines. Interestingly, cell size and shape in leaf parenchyma were different in C3 line. In particular, cells from this line were larger than those of control and they were not organized in palisade and spongy parenchyma (Fig. 3D–F). In order to measure the growth rate of TGBp1 cells, calli were obtained from 11-week old fifth upper leaves from lines C3 and E2. After 25 d of growth and subsequent sub-culturing for another 20 d, transgenic callus exhibited significant reduced growth as compared to control calli (Table 2).

2.2. Chloroplasts morphology

C3 leaf cells have flattened-shaped chloroplasts exhibiting very little content of starch granules as compared to control cells (Fig. 3D, E). In addition, dense globular structures were observed inside the chloroplasts of TGBp1 cells upon examination with the electron microscope (insert, Fig. 3E, F). These elements resembled plastoglobuli, a type of osmophilic elements that are commonly present in chloroplasts of senescent cells [16,36]. Analogous elements were observed in E2 leaves, but in lesser degree (insert, Fig. 3F). In agreement with a previous report on PVX-infected plants [7], TGBp1 localizes in cytoplasmic inclusion bodies in transgenic plants (data not shown).

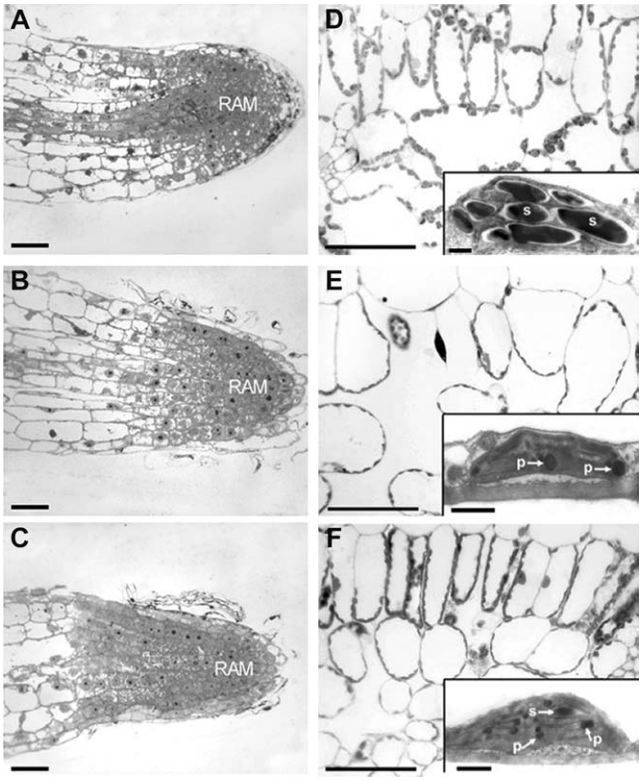

Fig. 3. LM and transmission electron microscopy (TEM) observations of control and transgenic plants RAM and leaves. **A–C**, RAM of C3 (**B**) and E2 (**C**) transgenic lines exhibit smaller RAM diameter as compared to *N. tabacum* Xanthi D8 (**A**). **D–F**, Chloroplasts of D8 cells show a normal morphology (**D**), while those of C3 (**E**) and E2 (**F**) cells exhibit a less spherical shape. Representative chloroplast structures are shown in the respective inserts. Starch grains (s) are clearly visible in D8 chloroplasts (insert **D**). Starch deposits are very small or absent and plastoglobuli are frequently observed (p) in C3 and E2 chloroplasts, respectively (**E** and **F** inserts). Bars: LM photographs = 50 μm (**A–F**); TEM photographs (**D–F** inserts) = 1 μm.

Table 2
Growth rate of TGBp1 calli. Calli derived from C3, E2 and *N. tabacum* Xanthi D8 control lines after 20 d growth. Average weights for calli corresponding to the different lines were determined and indicated as the percentage of D8 control callus weight (100%). The experiment was repeated three times with similar results

Plant	D8	E2	C3
Growth rate (%)	100	48.6 ** (6.3)	43.2 ** (9.6)

( ): Indicates standard deviation. ** $P < 0.01$ by Student's *t*-test.

2.3. Reduced carbohydrate levels in TGBp1 plants

Total carbohydrate content was lower in TGBp1 leaves as compared to controls (Fig. 4A). In particular, a pronounced decrease of starch contents was found in these plants. Given that total soluble sugars remain close to normal levels, this decrease resulted in an almost a threefold increase in the soluble-sugar-to-starch ratio. Roots of transgenic plants exhibited decreased soluble sugar levels. Since starch content was also lower in this organ, the soluble-sugar-to-starch ratio varies from three to fivefolds (Fig. 4B). Plants expressing the TGBp2 and TGBp3 genes did not show altered starch or soluble carbohydrate levels in leaves as compared to non-transgenic controls. However, minor reductions of total car-

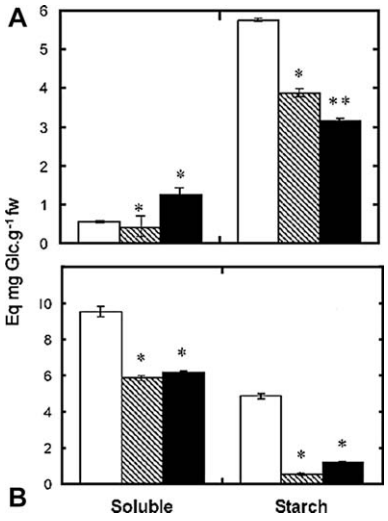

Fig. 4. Carbohydrate accumulation after a 7-h light period in leaves (**A**) and roots (**B**) of transgenic and control tobacco plants. Measurements were carried out in the fifth leaf of each plant at 13 weeks post-germination. Empty bars: *N. tabacum* Xanthi D8 control plants; right-stripped bars: E2 line plants; filled bars: C3 line plants. Standard deviations are indicated in each bar. Statistical significance: <0.05 (*) and <0.01(**) by Student's *t* analyses.

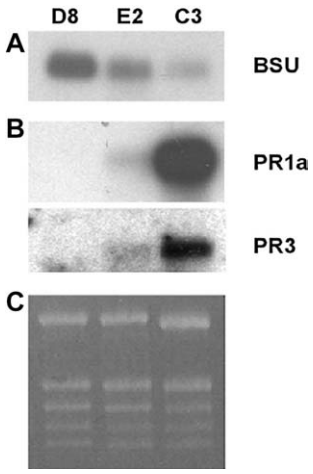

Fig. 5. Rubisco small subunit and PR gene expression in transgenic plants. Total RNA from transgenic (C3 and E2) and *N. tabacum* Xanthi D8 (D8) plants were extracted at 13 weeks post-germination and probed with P^{32}-labeled cDNA fragments containing Rubisco small subunit (BSU) or PR1a and PR3 sequences (**A** and **B**, respectively). Northern blot analyses were carried out on the same blot. RNA loading control stained with ethidium bromide (**C**). Five micrograms of total RNA from the third leaves of each plant were loaded in each lane.

bohydrate levels were observed in roots of TGB2 and TGB3 plants.

2.4. Photosynthetic rate in TGBp1 plants

In order to establish whether the reduced carbohydrate level found in TGBp1 plants was associated with alterations in their photosynthetic capacity, the CO_2 assimilation rate was measured. As shown in Table 3, photosynthetic rates were significantly reduced in TGBp1 plants, but not in TGBp2 and TGBp3 plants. However, respiration rates were similar in both transgenic and control plants, thus yielding higher respiration to photosynthesis (*R*/*P*) ratios in TGBp1 plants. Photosynthetic electron transport was also evaluated. The variable-to-maximal chlorophyll fluorescence ratio (F_v/F_{max}) in TGBp1 plants was close to the value obtained for control plants, suggesting that photosystem II (PS2) is not altered in these plants. However, the estimated electron transfer efficiency was slightly—but significantly—decreased in both lines (data not shown).

Reduction of photosynthetic capacity could also be consequence of down-regulation of photosynthetic genes [18,19], a fact that is usually observed during normal leaf senescence or as a result of sugar accumulation [12,30]. To test this possibility, a Northern blot analysis was conducted to evaluate transcription of the Rubisco small subunit gene. As shown in Fig. 5A, Rubisco mRNA accumulation was reduced in both TGBp1 lines.

2.5. Nitrate accumulation in TGBp1 plants

To explore whether the lower carbon assimilation induced by the decrease in the photosynthetic rate could be affecting assimilation of other metabolites in TGBp1 plants, nitrate content was measured in their leaves. As shown in Fig. 6, higher levels of nitrate accumulation were found in both transgenic lines. In particular, C3 third leaf samples showed a 10-fold increase in nitrate level.

2.6. Expression of pathogenesis-related (PR) protein genes in TGBp1 plants

PR proteins are typically induced during plant defense responses. In addition, different PR proteins were shown to

Table 3
Photosynthesis and respiration rates in TGBp1 and control plants. CO_2 flux was measured as described in Section 4. Values represent the average of quadruplicate measurements from a single representative experiment. Results are expressed as the mean value obtained from four individual of each plant line. The experiment was repeated three times with similar results. P8: tobacco line expressing the TGBp3 sequence. P12: tobacco line expressing the TGBp2 sequence

Plant	Photosynthesis (μl h^{-1} cm^{-2})	Respiration (μl h^{-1} cm^{-2})	*R*/*P* ratio over a 24 h period
D8	31.0 (2.0)	12.0 (1.5)	0.28
E2	16.5 * (1.5)	12.0 (1.5)	0.52
C3	14.5 * (1.5)	11.0 (1.0)	0.54
P8	33.0 (3.0)	11.0 (1.5)	0.24
P12	23.0 (4.0)	11.0 (2.0)	0.34

( ): Indicates standard deviation. * $P < 0.05$ by Student's *t*-test.

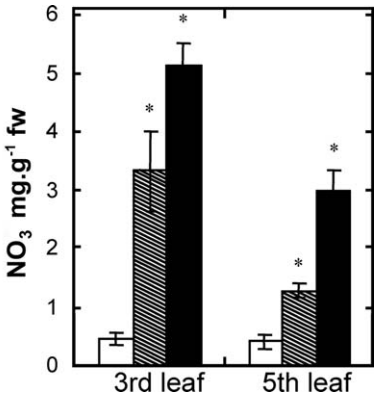

Fig. 6. Steady-state level of nitrate in transgenic and control plants. Samples corresponding to the third and fifth leaves were taken for nitrate measurements. Empty bars: *N. tabacum* Xanthi D8 control plants; right-stripped bars: E2 line plants; filled bars: C3 line plants. Standard deviations are indicated in each bar. Statistical significance <0.05 (*) by Student's *t* analysis.

be induced in plants engineered to accumulate sugars in their leaves [11,12], as well as in mutant and transgenic plants exhibiting different metabolic perturbations [3,10,26,35]. A Northern analysis of PR mRNAs showed that both PR1a and PR3 mRNAs were highly expressed in TGBp1 plants leaves (Fig. 5B). Expression of PR genes was not detected in other transgenic or non-transgenic plants (i.e. transgenic TGBp2, TGBp3, replicase and coat protein plants, non-transgenic plants and PVX-infected non-transgenic plants) ([17] data not shown).

3. Discussion

This is the first report describing the pleiotropic effects caused by transgenic expression of PVX TGBp1 in tobacco plants. Plants showing high and intermediate levels of transgenic protein exhibited consistent smaller sizes, shorter internodes, reduced leaf number and chlorotic phenotype. Development of this phenotype was correlated with TGBp1 accumulation in most transgenic lines (Table 1). It is worth noticing that TGBp1 plants showed a normal life cycle (i.e. germination, growth, and flowering times similar to that of non-transgenic controls). In addition, the shoot-to-root ratio was similar to that of non-transformed plants. This suggests that biomass partition in TGBp1 plants are not altered, as it seems to be the case of transgenic tobacco plants expressing the Tobacco mosaic virus p30 MP [24,28].

Biochemical studies performed in two representative TGBp1 lines showed consistent alterations in carbohydrate accumulation. Decreased starch contents in leaves and roots and significant reductions of soluble sugars in roots were found in both lines (Fig. 4). Although it is clear that TGBp1 accumulation influences host carbohydrate metabolism, no obvious explanation was found regarding the mechanisms involved in this effect. The decays observed in the photosynthetic rate seem to be associated with morphological alterations of chloroplasts within TGBp1 expressing lines, which showed diminished starch deposits and contained electron-dense bodies—presumably plastoglobuli—in their stroma. An increase in the number of plastoglobuli has been associated to chloroplast senescence [16,30,38] and progress of this process leads to loss of photosynthetic capacity and/or membrane integrity [4]. Interestingly, no co-localization of TGBp1 in chloroplast structures was found ([7] results not shown). Hence, the alterations observed in TGBp1 chloroplasts should be endorsed to an indirect effect of TGBp1 accumulation. Based on these findings, we conclude that the mechanisms operating in TGBp1 plants are different from those acting in plants transformed with other viral MPs, such as Potato leaf roll virus p17, in which the decrease of the photosynthetic rate is apparently mediated by high sugar concentrations and down-regulation of photosynthetic genes [12,13].

It has been previously demonstrated that induction of PR genes can result from high carbohydrate accumulation in leaf cells [34]. However, despite the lack of carbohydrate accumulation in TGBp1 leaves, PR genes were over-expressed in TGBp1 plants. Since PR genes expression is not observed during normal PVX infection of tobacco plants ([17] data not shown), this could be conceivably derived from TGBp1 over-expression in transgenic plants. As proposed by Dietrich et al. [8], this effect could be a consequence of an altered biochemical state resulting from abnormal chloroplast functioning. Accumulation of TGBp1 since very early developmental stages could enhance this process.

The reduced size of root meristems observed in TGBp1 seedling suggests that the decreased plant growth is associated to reduced meristem development. Supporting this, calli derived from transgenic plants exhibit reduced growth rates, indicating that cell proliferation is also lower in non-differentiated tissue. Since plasmodesmata are not fully established at this stage, this could imply a specific TGBp1 activity at the cell division level.

Based on these results, we presume that the stunted phenotype and the metabolic alterations observed in TGBp1 plants are derived from two independent effects of TGBp1: (*a*) an effect on proliferating tissues, such as root meristems, resulting in diminished cell division and plant size reductions; (*b*) a perturbation of normal chloroplast functioning leading to decreased photosynthesis and reduced carbohydrate accumulation. Since dwarfism in TGBp1 plants is established before the onset of photosynthetic activity, reduced photosynthesis could not explain the smaller size observed in young seedlings and their root meristems (Fig. 1B, C). Supporting this, transgenic *Arabidopsis thaliana* plants constitutively expressing TGBp1 also showed consistent growth reductions that correlate with TGBp1 accumulation, but do not reveal metabolic alterations or constitutive PR gene expression (data not shown; manuscript in preparation). Till present, the PVX TGBp1 has been shown to fulfill at least two major functions in viral infection: the promotion of cell-to-cell viral movement [1,22] and the suppression of post-transcriptional gene silencing [37]. Since both activities

could affect normal macromolecular traffic—and, consequently, developmental and metabolic signalization—, further studies will be needed to explore whether development of the TGBp1 phenotype is dependent on them or whether a novel function, also associated to this protein, is involved in this process.

Plant stunting and metabolic changes are commonly associated to plant virus diseases. Considering the fact that no other PVX protein induces abnormal phenotypes in transgenic plants, we propose that TGBp1, either by itself or in combination with other viral proteins, is an important symptom contributor in infections caused by this virus. Additional studies on cell division rates in TGBp1 tissues, co-expression of TGBp1 with other PVX proteins, and expression of TGBp1 in other species will help to further clarify these particular effects.

4. Methods

4.1. Virus isolates

Potato virus X strain CP2 (PVX-CP2) was obtained from the International Potato Center (Lima, Perú). Cloning and sequencing of the respective genomic sequence was previously reported ([29] GeneBank accession no. **X55802**).

4.2. Plant material and growth conditions

Nicotiana tabacum cv. Xanthi D8 NN used to generate transgenic plants was obtained from Y. Chupeau (INRA, Versailles, France). With the exception of those involved in gas exchange and chlorophyll fluorescence measurements (see below), all experiments were carried out on 10–11-week-old plants. A5, B16, C3, C6, D3 and E2 are tobacco transgenic lines constitutively expressing PVX TGBp1 [2]. C3 and E2 contain a single copy of the transgene and were self-pollinated to attain homozygocity. Transgenic p12-3 line was previously described [17]. Transgenic TGBp3 plants were obtained by transformation via *Agrobacterium tumefaciens* with a pBI121 binary expression vector (Clontech, USA) carrying the PVX TGBp3 sequence downstream of the 35S cauliflower mosaic virus promoter. Except where explicitly stated, only homozygous T2 plants were used in all experiments. All plants were individually grown on vermiculite in a growth chamber under a 14 h light/10 h dark regime (25 °C light/21 °C dark) at a light intensity of 300 μmol m^{-2} s^{-1} and automatically immersed in a Coic–Lesaint [6] mineral medium during 20 min everyday. Tobacco calli from transgenic and control plants were obtained from fifth leaf explants of about 1 cm^2 area and 0.2 g average weight. Twenty-five leaf explants of E2 and C3 transgenic lines and control D8 plants were excised and surface-sterilized following a standard procedure, and in vitro cultured in medium containing Murashige and Skoog salts and organics (Invitrogen, USA) supplemented with 3% sucrose, 1.5 mg l^{-1} 2,4-dichlorophenoxyacetic acid and 0.7% agar to induce calli formation. After 25 d, equivalent weights (0.6 g) of calli corresponding to the different plant lines were subcultured for 20 more days. Finally, fresh calli weights were measured and compared.

4.3. Northern and Southern blot analyses

Northern and Southern blot analyses were conducted as previously described in [17]. Tobacco cDNA sequences used for the study of PR1a, PR2 and PR3 mRNA expression were kindly provided by E. Lamb (Rutgers University, USA). The cDNA sequence corresponding to the *N. sylvestris* small Rubisco subunit (407 bp; GeneBank accession no. **X53426**) was amplified by PCR using oligonucleotides 5′-TCCC TGTTTCCAGGAAACAAA-3′ and 5′-CTTGTAGGCGA TGAAACTAAT-3′ as primers.

4.4. Western blot analysis

Western blot analysis was performed as described in [2]. TGBp1 was detected with rabbit antibodies raised against purified recombinant TGB1 protein [2]. Specifically bound antibodies were visualized by incubation with alkaline phosphatase-linked goat anti-rabbit antibodies followed by a chromogenic reaction using nitroblue tetrazolium and 5-bromo-4 chloro-3 indolyl phosphate (Promega, USA) as substrates.

4.5. Microscopical observations

Tobacco root and leaf samples of about 1 mm × 1 mm were fixed with 2.5% glutaraldehyde in 0.1 M phosphate buffer (pH 6.8), for 2 h at room temperature. Light microscopy (LM) was performed as previously described [17]. For electron microscopy, the tissue was post-fixed with 1% OsO_4 in distilled water for 1–2 h at 4 °C, dehydrated in a graded ethanol-propylene oxide series and embedded in Spurr's resin (Polyscience, USA). Thin sections were prepared using an Ultracut E microtome (Reichert-Jung, Germany). Tissue sections were mounted on grids coated with Formward (Polyscience, USA) and carbon, and then stained in uranyl acetate followed by lead citrate. Sections were observed under a Zeiss EM 10C (Carl Zeiss, Germany) transmission electron microscope.

4.6. Gas exchange measurements

Six- to 7-week-old tobacco plants were used for the experiments. The photosynthetic rate was calculated during the light period as the quantity of CO_2 fixed per unit of leaf area. CO_2 exchange measurements were performed in twin airtight environmental chambers with light intensity adjusted at 300 μmol m^{-2} s^{-1}. CO_2 concentration was measured with a Miahak Finor IRGA (Hamburg, Germany) CO_2 analyzer. The CO_2 molar ratio was maintained at 350 ± 2 μmol CO_2

mol^{-1} air using pulsed injections of CO_2 controlled by a computer. During the dark period, CO_2 level was regulated by passing air through a soda lime trap. Whole-plant respiration was calculated from the time of passage through the trap. Respiration rate was normalized to total leaf area.

4.7. Metabolite analysis

For sugars and starch analysis, samples (1 g of leaf tissue) from fifth upper leaves was extracted in liquid nitrogen with 2 ml of 10 mM Tris–HCl buffer (pH 7.4). After a brief centrifugation at 11,900 × *g*, soluble sugars were measured on the supernatant using a commercial kit (Boehringer-Mannheim, Germany). For starch measurements, the pellet was resuspended in 1 ml of 0.5 M NaOH for 1 h at 60 °C, followed by addition of 20 μl of 3 M sodium acetate/acetic acid (pH 4.5) and 80 μl of 5 N HCl. Starch was determined using a commercial kit (Boehringer-Mannheim) and expressed as glucose equivalents. A similar procedure was followed for nitrate analysis; in this case, 2 ml of distilled water were used to resuspend the pellet. After a brief centrifugation at 11,900 × *g*, nitrate was measured on the supernatant using the procedure described by Castaldo et al. [5].

4.8. Chlorophyll fluorescence measurements

Chlorophyll fluorescence measurements were conducted with a PAM-2000 fluorometer (Walz, Germany) on complete fifth upper leaves taken from 6- to 7-week-old plants. Maximum quantum yield of photosystem II was measured by estimating the F_v to F_{max} ratio in leaves adapted for 30 min to the dark. $F_v = F_{max} - F_0$, in which F_v is the variable chlorophyll fluorescence, F_{max} is the maximal level of chlorophyll fluorescence induced by pulse of white light (photon flux density > 4000 μmol m^{-2} s^{-1}) of 800 ms and F_0 is the initial level of fluorescence under red light (655 nm) modulated at 600 Hz. The effective quantum yield was calculated from chlorophyll fluorescence measured on leaves continuously illuminated at 255 and 600 μmol m^{-2} s^{-1} treated with regular pulses of saturating light to estimate the electron transfer efficiency. Results are shown as average values from three individual plants per line.

Acknowledgements

We wish to thank Séverine Boiry and Michel Péan for their assistance with plant growth chambers. This work was partially supported by Grant No. 2851/98-4 of CONICET, Argentina and Grant No. B02179 from MENRT, France. K.K. was supported by a fellowship of FOMEC/FCEyN-UBA. M.R. is a Teaching Assistant of FCEN-UBA. S.M. and A.M. are research scientists of CONICET, Argentina.

References

[1] S.M. Angell, C. Davies, D.C. Baulcombe, Cell-to-cell movement of potato virus X is associated with a change in the size-exclusion limit of plasmodesmata in trichome cells of *Nicotiana clevelandii*, Virology 216 (1996) 197–201.

[2] X. Ares, G. Calamante, S. Cabra, J. Lodge, P. Hemenway, R.N. Beachy et al., Transgenic plants expressing potato virus X ORF2 protein (p24) are resistant to tobacco mosaic virus and Ob tobamoviruses, J. Virol. 72 (1998) 731–738.

[3] F. Becker, E. Buschfeld, J. Schell, A. Bachmair, Altered response to viral infection by tobacco plants perturbed in ubiquitin system, Plant J. 3 (1993) 875–881.

[4] A.B. Bleeker, S.E. Patterson, Last exit: senescence, abscission, and meristem arrest in *Arabidopsis*, Plant Cell 9 (1997) 1169–1179.

[5] D.A. Castaldo, M. Haroon, L.E. Schrader, V.L. Youngs, Rapid colorimetric determination of nitrate in plant tissue by titration of salicylic acid, Commun. Soil Sci. Plant Anal. 6 (1975) 71–80.

[6] E.C. Coic, C. Lesaint, Comment assurer une bonne nutrition en eau et éléments minéraux en horticulture, Hortic. Fr. 8 (1971) 11–14.

[7] C. Davies, G. Hills, D.C. Baulcombe, Sub-cellular localization of the 25-kDa protein encoded in the triple gene block of potato virus X, Virology 197 (1993) 166–175.

[8] R.A. Dietrich, T.P. DeLaney, S.J. Uknes, E.R. Ward, J. Ryals, J.L. Dangl, *Arabidopsis* mutants simulating disease resistance response, Cell 77 (1994) 565–574.

[9] T.M. Foster, T.J. Lough, S.J. Emerson, R.H. Lee, J.L. Bowman, R.L.S. Forster, W.J. Lucas, A surveillance system regulates selective entry of RNA into the shoot apex, Plant Cell 14 (2002) 1497–1508.

[10] C. Hanfrey, M. Fife, V. Buchanan-Wollaston, Leaf senescence in *Brassica napus*: expression of genes encoding pathogenesis-related proteins, Plant Mol. Biol. 30 (1996) 597–609.

[11] K. Herbers, P. Meuwly, J.P. Metraux, U. Sonnewald, Salicylic acid-independent induction of pathogenesis-related protein transcripts by sugars is dependent on leaf developmental stage, FEBS Lett. 397 (1996) 239–244.

[12] K. Herbers, E. Tacke, M. Hazirezaei, K.P. Krause, M. Melzer, W. Rohde et al., Expression of luteoviral movement protein in transgenic plants leads to carbohydrate accumulation and reduced photosynthetic capacity in source leaves, Plant J. 12 (1997) 1045–1056.

[13] D. Hofius, K. Herbers, M. Melzer, A. Omid, E. Tacke, S. Wolf, U. Sonnewald, Evidence for expression level-dependent modulation of carbohydrate status and viral resistance by the potato leaf roll virus movement protein in transgenic tobacco plants, Plant J. 28 (2001) 529–543.

[14] M.J. Huisman, H.J.M. Linthorst, J.F. Bol, B.J.C. Cornelissen, The complete nucleotide sequence of potato virus X and its homologies at the amino acid level with various plus-stranded RNA viruses, J. Gen. Virol. 69 (1988) 1789–1798.

[15] N.O. Kalinina, O.N. Fedorkin, O.V. Samuilova, E. Maiss, T. Korpela, S. Morozov et al., Expression and biochemical analyses of the recombinant potato virus X 25K movement protein, FEBS Lett. 397 (1996) 75–78.

[16] F. Kessler, D. Schnell, G. Blobel, Identification of proteins associated with plastoglobules isolated from pea (*Pisum sativum* L.) chloroplasts, Planta 208 (1999) 107–113.

[17] K. Kobayashi, S. Cabral, G. Calamante, S. Maldonado, A. Mentaberry, Transgenic tobacco plants expressing potato virus X ORF3 gene develop specific resistance and necrotic ring symptoms after infection with the homologous virus, Mol. Plant–Microbe Interact. 11 (2001) 1274–1285.

[18] A. Krapp, B. Hofmann, C. Schäfer, M. Stitt, Regulation of the expression of *rbcS* and other photosynthetic genes by carbohydrates: a mechanism for the "sink-regulation" of photosynthesis? Plant J. 3 (1993) 817–828.

[19] A. Krapp, M. Stitt, An evaluation of direct and indirect mechanisms for the sink-regulation of photosynthesis in spinach: changes in gas exchange, carbohydrates, metabolites, enzyme activities and steady-state transcript levels after cold-girdling source leaves, Planta 195 (1995) 13–23.

[20] K. Krishnamurthy, M. Heppler, R. Mitra, E. Blancaflor, M. Payton, R.S. Nelson, J. Verchot-Lubicz, The potato virus X TGBp3 protein associates with the ER network for virus cell-to-cell movement, Virology 309 (2003) 135–151.

[21] K. Krishnamurthy, R. Mitra, M.E. Payton, J. Verchot-Lubicz, Cell-to-cell movement of the PVX 12K, 8K, or coat proteins may depend on the host, leaf developmental stage, and the PVX 25K protein, Virology 300 (2002) 269–281.

[22] T.J. Lough, N.E. Netzler, S.J. Emerson, P. Sutherland, F. Carr, D.L. Beck, W.J. Lucas, R.L. Forster, Cell-to-cell movement of potexviruses: evidence for a ribonucleicprotein complex involving the coat protein and first triple gene block protein, Mol. Plant–Microbe Interact. 13 (2000) 962–974.

[23] T.J. Lough, K. Shash, B. Xoconostle-Cázares, K.R. Hofstra, D.L. Beck, E. Balmori et al., Molecular dissection of the mechanism by which potexvirus triple gene blocks mediate cell-to-cell transport of infectious RNA, Mol. Plant Microbe Interact. 11 (1998) 801–814.

[24] W.J. Lucas, A. Olesinski, R.S. Hull, J.S. Haudenshield, C.M. Deom, R.N. Beachy et al., Influence of the tobacco mosaic virus 30 kDa movement protein on carbon metabolism and photosynthesis partitioning in transgenic tobacco plants, Planta 190 (1993) 88–96.

[25] R. Mitra, K. Krishnamurthy, E. Blancaflor, M. Payton, R.S. Nelson, J. Verchot-Lubicz, The potato virus X TGBp2 protein association with the endoplasmic reticulum plays a role in but is not sufficient for viral cell-to-cell movement, Virology 312 (2003) 35–48.

[26] R. Mittler, V. Shulaev, E. Lam, Coordinated activation of programmed cell death and defense mechanisms in transgenic tobacco plants expressing a bacterial proton pump, Plant Cell 7 (1995) 29–42.

[27] S.Y. Morozov, A.G. Solovyev, Triple gene block: modular design of a multifunctional machine for plant virus movement, J. Gen. Virol. 84 (2003) 1351–1366.

[28] A.A. Olesinski, W.J. Lucas, E. Galun, S. Wolf, Pleiotropic effects of tobacco mosaic virus movement protein on carbon metabolism in transgenic tobacco plants, Planta 197 (1995) 118–126.

[29] B.E. Orman, R.M. Celnik, A.M. Mandel, H.N. Torres, A.N. Mentaberry, Complete DNA sequence of a South American isolate of potato virus X, Virus Res. 16 (1990) 293–305.

[30] F.B. Quirino, Y.-S. Noh, E. Himelblau, R. Amasino, Molecular aspects of leaf senescence, Trends Plant Sci. 5 (2000) 278–282.

[31] M. Rouleau, R.J. Smith, J.B. Bancroft, G.A. Mackie, Purification, properties, and subcellular localization of foxtail mosaic potexvirus 26-kDa protein, Virology 204 (1994) 254–265.

[32] M. Rouleau, R.J. Smith, J.B. Bancroft, G.A. Mackie, Subcellular immunolocalization of the coat protein of two potexviruses in infected *Chenopodium quinoa*, Virology 214 (1995) 314–318.

[33] A.G. Solovyev, T.A. Stroganova, A.A. Zamyatnin, O.N. Fedorkin, J. Schiemann, S.Y. Morozov, Subcellular sorting of small membrane-associated triple gene block proteins: TGBp3-assisted targeting of TGBp2, Virology 269 (2000) 113–127.

[34] V. Sonnewald, M. Brauer, A. Von Schaewen, M. Stitt, L. Willmitzer, Transgenic tobacco plants expressing yeast-derived invertase in either the cytosol, vacuole or apoplast: a powerful tool for studying sucrose metabolism and sink/source interactions, Plant J. 1 (1991) 95–106.

[35] M. Takahashi, K. Shimamoto, Y. Ehara, Cauliflower mosaic virus gene VI causes growth suppression, development of necrotic spots and expression of defense-related genes in transgenic tobacco plants, Mol. Gen. Genet. 216 (1989) 188–194.

[36] M. Tevini, D. Steinmuller, Composition and function of plastoglobuli. I. Lipid composition of leaves and plastoglobuli during beech senescence, Planta 163 (1985) 91–96.

[37] O. Voinnet, C. Lederer, D.C. Baulcombe, A viral movement protein prevents spread of the gene silencing signal in Nicotiana benthamiana, Cell 103 (2000) 157–162.

[38] H.W. Woolhouse, Regulation of senescence in the chloroplast, in: W.W. Thomson, E.A. Nothnagel, R.C. Huffaker (Eds.), Plant Senescence: Its Biochemistry and Physiology, American Society of Plant Physiologists, Rockville, 1987, pp. 132–146.

[39] Y. Yang, B. Ding, D.C. Baulcombe, J. Verchot, Cell-to-cell movement of the 25K protein of potato virus X is regulated by three other viral proteins, Mol. Plant–Microbe Interact 13 (2000) 599–605.